THE ASTRONOMICAL JOURNAL VOLUME 102, NUMBER 2 AUGUST 1991

HIGH REDSHIFT RADIO GALAXIES FROM THE MOLONGLO CATALOGUE. II

P. J. McCARTHY
The Observatories of the Carnegie Institution of Washington, 813 Santa Barbara Street, Pasadena, California 91101

W. VAN BREUGEL
Institute of Geophysics and Planetary Physics, Lawrence Livermore National Laboratory, Livermore, California 94550

V. K. KAPAHI AND C. R. SUBRAHMANYA
National Center for Radio Astronomy, Tata Institute of Fundamental Research, Poona University Campus, Ganeshkhind, Pune 41107, India
Received 11 March 1991; revised 26 April 1991

ABSTRACT

We report further results from our ongoing study of radio galaxies from the Molonglo Reference Catalogue. The sources were selected to have 408 MHz flux densities greater than 0.95 Jy and low frequency spectral indices steeper than -0.9. VLA 6 cm maps, optical identifications and redshifts for 18 sources are presented. Most of these sources are identified with faint galaxies, many of which have extended optical structures with morphologies characteristic of high redshift ($z > 1$) radio galaxies. Long slit spectroscopic observations have yielded redshifts for all of the galaxies, three of which have $z > 2$. Spectrophotometry of 1 Jy and the 3CR samples are used to distinguish between an L (emission line) versus L (radio) correlation as opposed to an L (emission line) versus redshift correlation. Our results strongly support an intrinsic L (emission line) versus L (radio) correlation. The structure of the sources in this, and other 1 Jy samples, are substantially different from the 3C sources, the 1 Jy galaxies having stronger cores and jets.

1. INTRODUCTION

Our knowledge of radio galaxies at large redshifts has increased markedly in the past few years, due to both the systematic study of complete samples and intensive observations of a few special objects. These studies have revealed a number of remarkable aspects of these young galaxies and their radio sources. Two results which are most difficult to reconcile are the strong alignment between the radio source and optical axes (McCarthy *et al.* 1987; Chambers *et al.* 1987) and the small dispersion of the K-band Hubble diagram (Lilly 1989). Recent reviews of this field are given by van Breugel & McCarthy (1990) and Chambers & Miley (1990).

A number of large surveys of radio galaxies at intermediate flux densities are now under way. The enormous effort expended by Spinrad and collaborators in completing the optical work on the 3CR sample illustrates the difficulty in carrying out all-sky (single hemisphere) unrestricted flux limited samples. Pursuing radio samples to levels significantly fainter than the 3CR clearly requires restrictions in addition to flux density to allow completion in a reasonable time. The B2/1 Jy (Allington-Smith *et al.* 1982) and the Parkes Selected Regions (Dunlop *et al.* 1988) are restricted only in sky coverage, while the 4C ultrasteep spectrum sample of Chambers *et al.* (1990) is restricted only by spectral index. The exact selection criteria employed in the various samples currently under study are determined in part by the goals of the individual investigators. Some are tailored to finding the highest redshifts, and so employ criteria designed to select a particular class of source, while others are aimed at assembling an unbiased view of the radio source population as a whole and therefore only employ sky coverage restrictions. Our survey has two primary goals. The first is to select a sample of radio galaxies in the same redshift range as the 3CR, but to lower radio luminosities. This may help us to differentiate between redshift and luminosity dependencies in the various radio-optical correlations found in the 3CR sample. The second goal is to increase the number of radio galaxies known with $z > 2$ (the effective limit of the 3CR). Our sources form a subset of the Molonglo Reference Catalog (Large *et al.* 1971) in a 10° strip in declination, centered at $\delta = -25°$. All of the sources in this strip with $S_{408\ \mathrm{MHz}} > 0.95$ Jy were observed at 843 MHz with the Molonglo Synthesis by Subrahmanya. We employ two further selection criteria to improve the likelihood of selecting sources with redshifts greater than ~ 0.5. These are (a) low frequency spectral indices steeper than -0.9 and (b) the lack of an optical identification (or a plate limit identification) on the SRC-J southern sky survey films at the 408 MHz Molonglo Reference Catalogue position. The motivations behind these particular selection criteria are given more fully in McCarthy *et al.* (1990; hereafter referred to as Paper I).

2. OBSERVATIONS

2.1 Radio Imaging

All of the radio sources were observed with the VLA at 6 cm with the array in its hybrid A/B configuration which is well suited to southern sources. Each source was observed for roughly 5 min at a single hour angle with frequent observations of calibrator sources interleaved. CLEANed and self-calibrated maps were made for each source using standard processing techniques.

The 6 cm maps of all of the sources that were observed spectroscopically are presented in Figs. 1(a)–1(r). The resolution varies between roughly 1".3 and 2" and the typical rms noise in each map is 0.15 mJy. We chose to use circular beams in the final maps for easier interpretation of small scale radio structure. In Table 1 we give the flux densities of

 0004-6256/91/020522-15$00.90

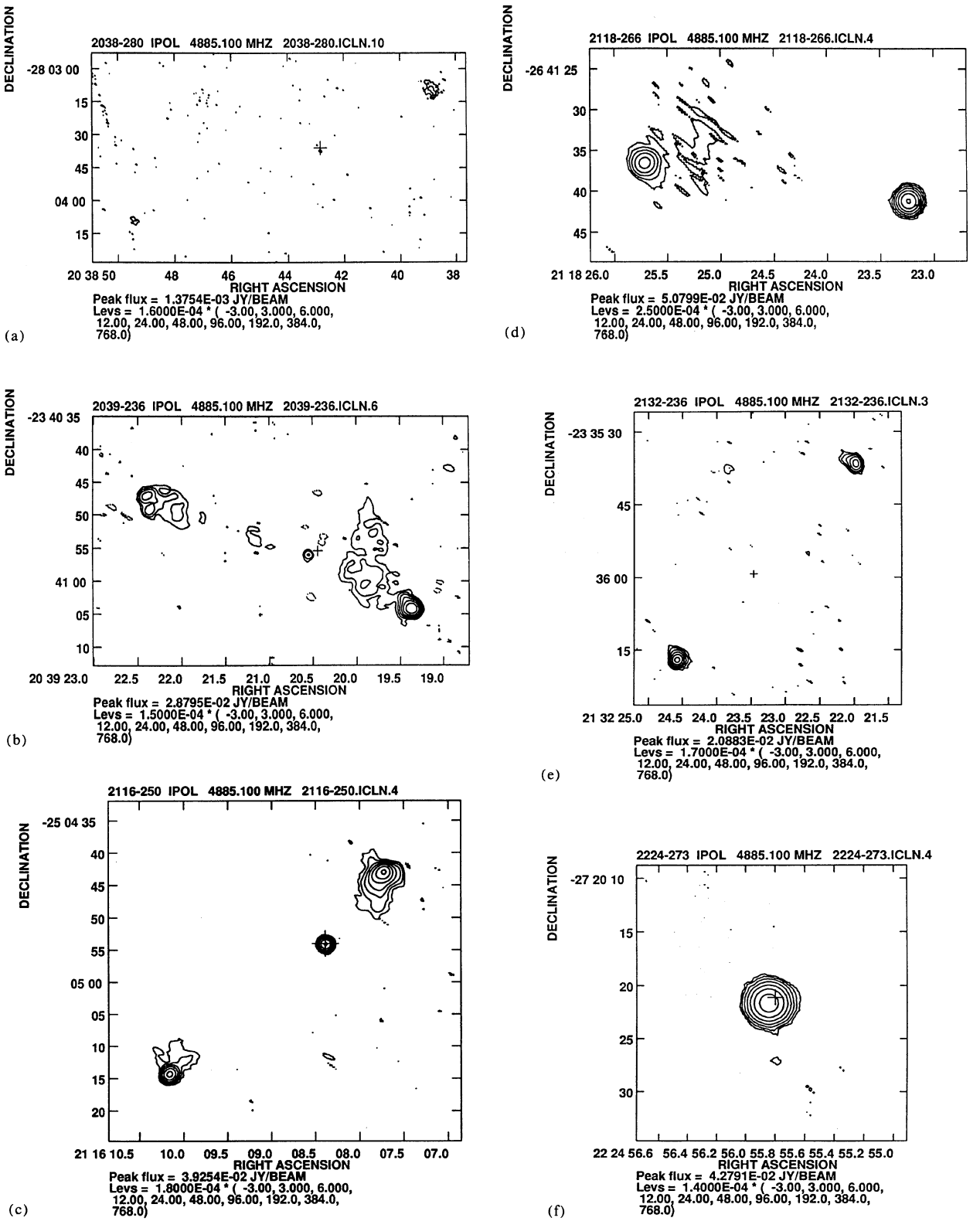

FIG. 1. (a)–(d) VLA 6 cm maps of 2038 – 280, 2039 – 232, 2116 – 250, and 2118 – 266. The average resolution of each map is 1.″3 and the position of the optical identification is marked with a cross. For each map the contours levels are – 3, 3, 5, 10, 20, 40, 80, 160, 320, and 640 times the rms noise per beam, which is typically 0.16 mJy. (e)–(h) 6 cm maps of 2132 – 236, 2224 – 273, 2227 – 214, and 2247 – 232. (i)–(l) 2318 – 244, 2321 – 228, 0140 – 257, and 0152 – 209. (m)–(p) 0254 – 274, 0324 – 228, 0325 – 260, and 0349 – 211. (q)–(r) 0406 – 244 and 0407 – 226.

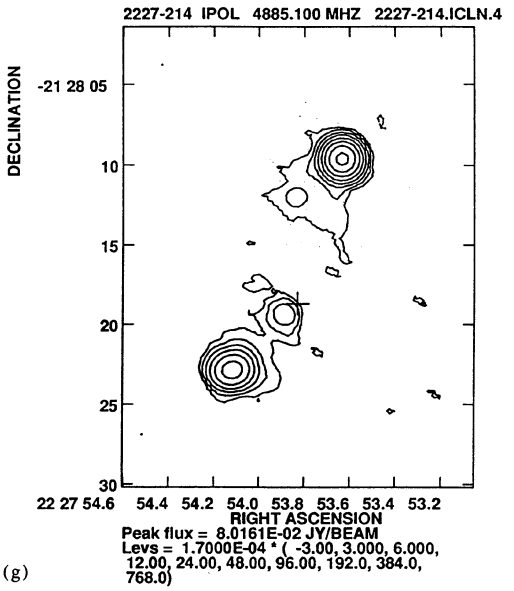

(g)

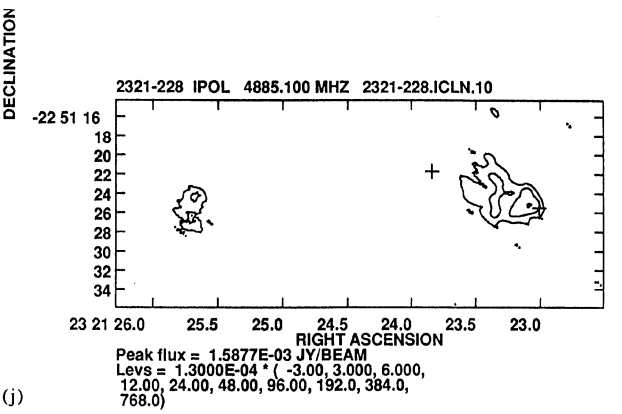

(j)

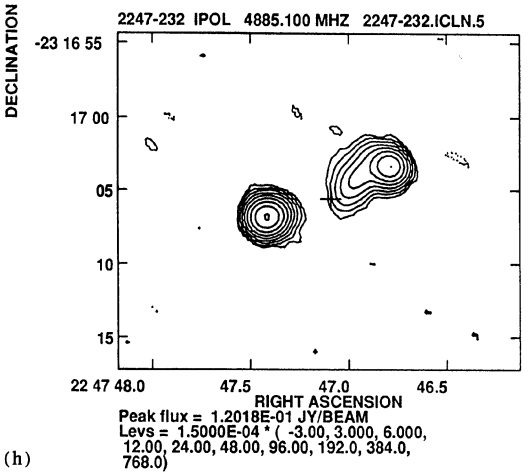

(h)

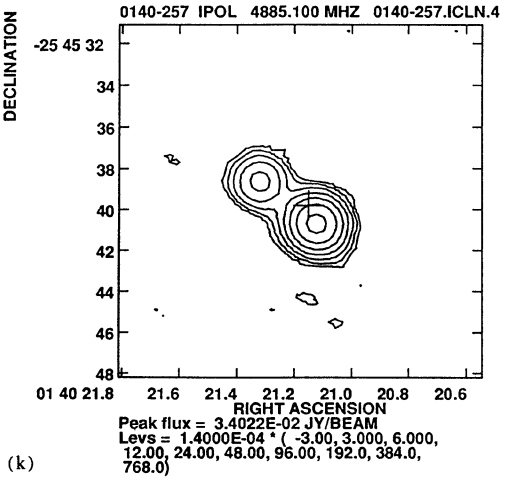

(k)

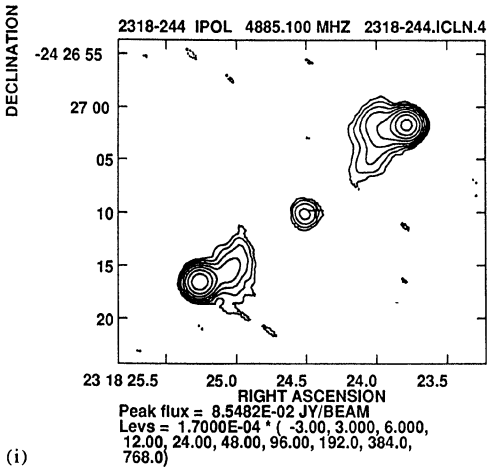

(i)

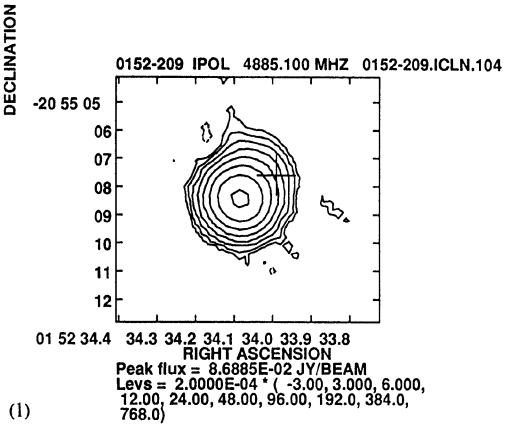

(l)

FIG. 1. (continued)

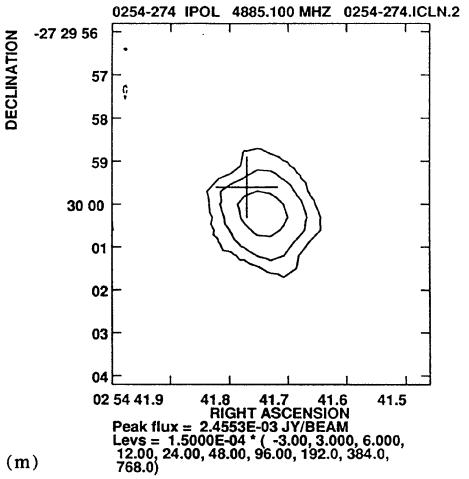

(m)

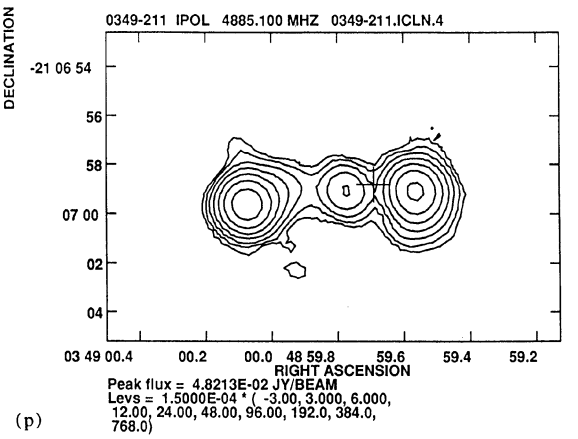

(p)

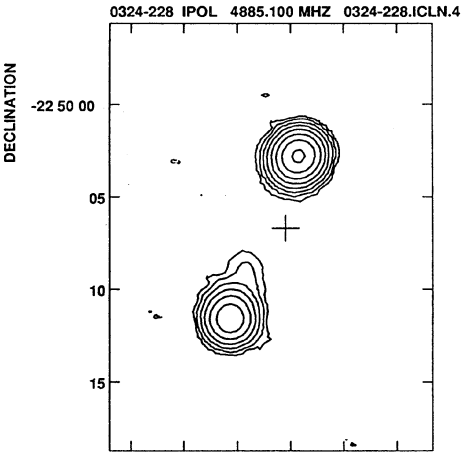

(n)

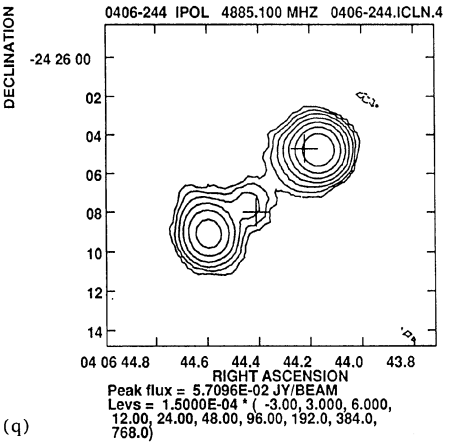

(q)

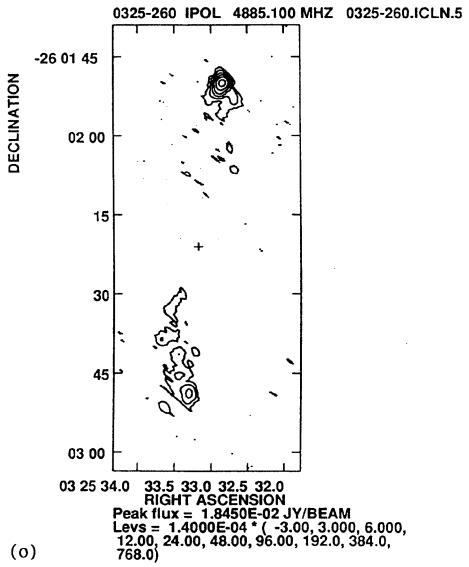

(o)

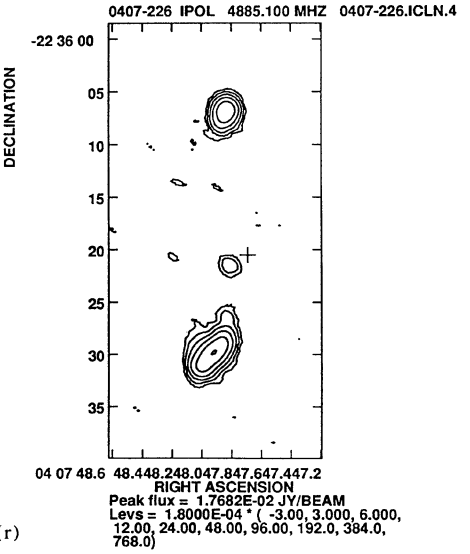

(r)

FIG. 1. (continued)

TABLE 1. Radio data.

Name	z	S_t(4.9) mJy	$Lobe_p$ mJy	$Lobe_f$ mJy	Core mJy	θ_t "	α	Log $P_{1.4}$ erg/s/Hz	Log L_R erg/s
2038-280	0.390	> 69	30.0	9.2	1.4	150	<1.23	>33.5	>43.73
2039-236	0.621	152.7	114.4	36.2	2.1	45	0.95	34.2	44.26
2116-250	0.467	168.1	110.5	38.1	19.5	46	0.94	33.9	43.98
2118-266	0.343	137.8	-	86.2	51.6	33	0.86	33.4	43.56
2132-236	0.810	57.1	22.6	34.5	-	55	1.14	34.1	44.30
2224-273	1.680	43.3	-	-	43.3	0.4	1.33	35.1	45.41
2227-214	1.410	142.8	102.0	37.4	3.4	15	1.02	35.1	45.22
2247-232	1.330	250.2	96.6	153.6	-	9.3	1.04	35.3	45.42
2318-244	1.120	217.3	128.1	83.7	5.5	25	0.97	35.0	45.08
2321-228	0.114	31.1	23.0	8.1	-	36	1.41	32.1	42.47
0140-257	2.640	42.4	33.9	8.5	-	3.4	1.28	35.7	45.95
0152-209	1.890	103.6	-	-	-	0.6	1.09	35.4	45.54
0254-274	0.480	> 27	-	-	2.6	1.3	<1.46	>33.5	>43.95
0324-228	1.890	104.0	74.2	29.8	-	9.5	1.19	35.5	45.71
0325-260	0.638	62.5	43.7	18.8	-	59	1.13	33.9	44.08
0349-211	2.310	113.7	45.9	60.7	7.1	7.1	0.93	35.6	45.66
0406-244	2.440	96.0	66.3	27.0	2.7	7.3	1.13	36.0	46.40
0407-226	1.480	82.0	25.5	54.5	2.0	23	1.10	35.0	45.14
2025-218	2.630	87.3	53.9	33.4	-	4.0	1.09	35.7	45.83
2028-293	0.500	114.9	57.7	57.2	-	4.9	1.01	33.9	44.00
2104-242	2.490	63.6	11.3	52.3	-	21.6	1.32	35.9	46.05
2115-253	1.114	61.4	44.1	17.3	-	1.6	1.19	34.7	44.87
2200-252	-	94.3	44.6	49.7	-	11.4	1.05	-	-
2226-224	0.380	121.0	51.4	59.6	10.0	10.6	0.93	33.4	43.56
2247-248	1.630	99.7	45.1	32.7	21.9	13.2	0.95	35.0	45.13
2303-253	0.730	153.6	93.9	57.4	2.3	18.8	1.08	34.6	44.67
0030-219	2.168	75.4	-	-	75.4	< 0.3	1.08	35.3	45.44
0034-235	-	96.9	40.2	56.7	-	15.6	1.15	-	-
0156-252	2.090	103.4	6.9	81.0	15.5	6.6	1.05	35.5	44.26
0203-209	1.257	67.9	15.4	48.2	4.3	12.1	1.13	34.7	44.82
0316-257	3.13:	92.3	57.0	35.3	-	6.7	1.03	36.1:	46.19:

Notes to TABLE 1

The first half of the table contains data for the newly identified sources. The second half contains data for sources whose identifications were presented in Paper I.

Cols. 3–6. 4.9 GHz flux densities as determined from the VLA maps. (t = total; p = north preceding lobe; f = north following lobe.) Uncertainties are typically ~5%, or ~0.5 mJy (which is larger), except for sources that are heavily resolved. For these sources limits were determined from the visibility curves. Compact core flux densities (and sizes) were determined using a Gaussian deconvolution program in the NRAO/AIPS data reduction package. For these the uncertainties are typically ~5%, or ~0.1 mJy (whichever is larger).

Col. 7. The largest angular extent of the radio source components are measured from the maps.

Col. 8. Spectral index ($S_\nu \sim \nu^{-\alpha}$) between 4.9 GHz (VLA) and 408 MHz (Molonglo). Upper limits are due to missing flux density in heavily resolved sources.

Col. 9. Rest frame 1400 MHz radio power determined for $H_0 = 50$, and $q_0 = 0$.

Col. 10. total radio luminosity for $10^7 < \nu < 10^{11}$ Hz.

the individual source components, the maximum angular extent, and spectral index at 1400 MHz and the rest-frame flux density and power at 1400 MHz. The 1400 MHz spectral indices are determined from our VLA 4.9 GHz flux densities and the MRC 408 MHz measurements. In the last column of Table 1 we give the source luminosity integrated from 10 MHz to 100 GHz using the 1400 MHz spectral indices. The derived radio positions are given in Table 2. For sources without detected central components, we list the midpoint between the two hotspots rather than the flux density weighted centroid.

2.2 Optical Imaging

Deep optical images were obtained with the Las Campanas 2.5 m Du Pont telescope in October 1989 and August 1990. Each field was observed with a Gunn–Thuan r filter. Several short integrations (300–900 s) were made and combined to give total integration times of typically 2400 s. The observing conditions were photometric, but the seeing was often mediocre (1.4–1.8 FWHM). The detector was either a TI 800×800 CCD used in a 2×2 on-chip binning mode to give 0".331 pixels or a Tektronics 512×512 with 0".29 pixels. The optical images were flattened using dark sky flats and were calibrated using standard techniques. Individual processed images of each field were shifted into registration and added. The radio sources were identified from astrometry of stars in each field whose positions were determined relative to a grid of SAO stars from the POSS. The typical rms errors of the primary astrometric solutions were 0".7 in each coordinate. The final rms errors for the derived galaxy positions are roughly 1". Of the 18 sources presented here one was identified with a Quasar, five with relatively bright galaxies ($r\sim18$–20), and the remaining 12 were identified with galaxies fainter than $r=20$. The photometry was performed with 4" diameter apertures and was calibrated using standard stars photometered by I. Thompson and L. Searle. The positions for each of the optical identifications (designated by O) are listed in Table 2, along with the position of a bright secondary reference star (A or B). Grey scale reproductions of each field are presented in Figs. 2(a)–2(p). Each field shown in Fig. 2 is $65''\times65''$, except for 0254 − 274 for which the field is $130''\times130''$. In each image the position of the identification is marked by two lines, the orientation of which reflects the position angle of the extended radio source. A secondary reference star is identified by a capital "A" or "B" in each field.

2.3 Optical Spectroscopy

Spectroscopic observations were made with the Cerro Tololo 4 m telescope and its Folded–Schmidt spectrograph on 22, 23, and 24 August 1990 (UT). We used a 150 line/mm grating blazed at 4000 Å covering the wavelength range from 3100 to 6500 Å. The average pixel size was 4.3 Å$\times$0.55". For each galaxy observed, we offset the telescope from the secondary reference star listed in Table 2. Typical integration times were 2500–3000 s. Thin cirrus clouds were present during most of 23 August, the other two nights were photometric. Observations of He-Ne-Ar lamps and spectrophotometric standard stars from Oke (1974) were made to calibrate the data.

Spectroscopic observations of the brighter galaxies were made in the red with the Du Pont telescope and its Modular

TABLE 2. Astrometric data.

IAU Name		α(1950)			δ(1950)			
2038-280	O	20	38	42.84	-28	03	35.9	
	R	20	38	42.84	-28	03	37.3	core
	A	20	38	40.49	-28	03	46.0	
2039-232	O	20	39	20.44	-23	40	55.4	
	R	20	39	20.55	-23	40	56.0	core
	A	20	39	25.04	-23	40	52.9	
2116-250	O	21	16	08.36	-25	04	53.0	
	R	21	16	08.38	-25	04	54.1	core
	A	21	16	09.29	-25	04	40.8	
2118-266	O	21	18	23.12	-26	41	41.8	
	R	21	18	23.24	-26	41	41.2	core
	A	21	18	26.77	-26	41	20.3	
2132-236	O	21	32	23.46	-23	35	59.3	
	R	21	32	23.29	-23	35	57	center
	A	21	32	23.46	-23	35	22.6	
2224-273	O	22	24	55.80	-27	20	21.1	
	R	22	24	55.84	-27	20	21.6	core
	B	22	24	55.71	-27	19	59.4	
2227-214	O	22	27	53.83	-21	28	18.7	QSR
	R	22	27	53.89	-21	28	19.4	core
	A	22	27	52.97	-21	28	54.6	
2247-232	O	22	47	47.09	-23	17	05.6	
	R	22	47	47.10	-23	17	04.6	center
	A	22	47	47.96	-23	17	07.8	
2318-244	O	23	18	24.43	-24	27	09.8	
	R	23	18	24.51	-24	27	10.1	core
	A	23	18	26.86	-24	26	20.8	
2321-228	O	23	21	23.82	-22	51	21.6	
	R	23	21	24.46	-22	51	24.2	center
	A	23	21	21.46	-22	51	11.5	
0140-257	O	01	40	21.15	-25	45	39.8	
	R	01	40	21.20	-25	45	39.6	center
	A	01	40	20.25	-25	45	44.1	
0152-209	O	01	52	33.99	-20	55	07.6	
	R	01	52	34.08	-20	55	08.4	center
	A	01	52	34.04	-20	55	06.8	
0254-274	O	02	54	41.77	-27	29	59.6	
	R	02	54	41.75	-27	30	00.2	core:
	B	02	47	47.96	-27	29	52.1	
0324-228	O	03	24	52.62	-22	50	06.7	
	R	03	24	52.68	-22	50	15.1	center
	A	03	24	53.73	-22	51	03.7	
0325-260	O	03	25	33.18	-26	02	21.1	
	R	03	25	33.14	-26	02	18.6	center
	A	03	25	32.56	-26	02	01.0	
0349-211	O	03	48	59.69	-21	06	58.8	
	R	03	48	59.77	-21	06	59.1	core
	A	03	48	59.57	-21	06	53.1	
0406-244	O	04	06	44.41	-24	26	08.0	
	O	04	06	44.22	-24	26	04.7	
	R	04	06	44.44	-24	26	07.6	core
	A	04	06	43.67	-24	26	19.5	
0407-226	O	04	07	47.69	-22	36	20.5	
	R	04	07	47.81	-22	36	21.5	core
	B	04	07	50.87	-22	36	11.2	

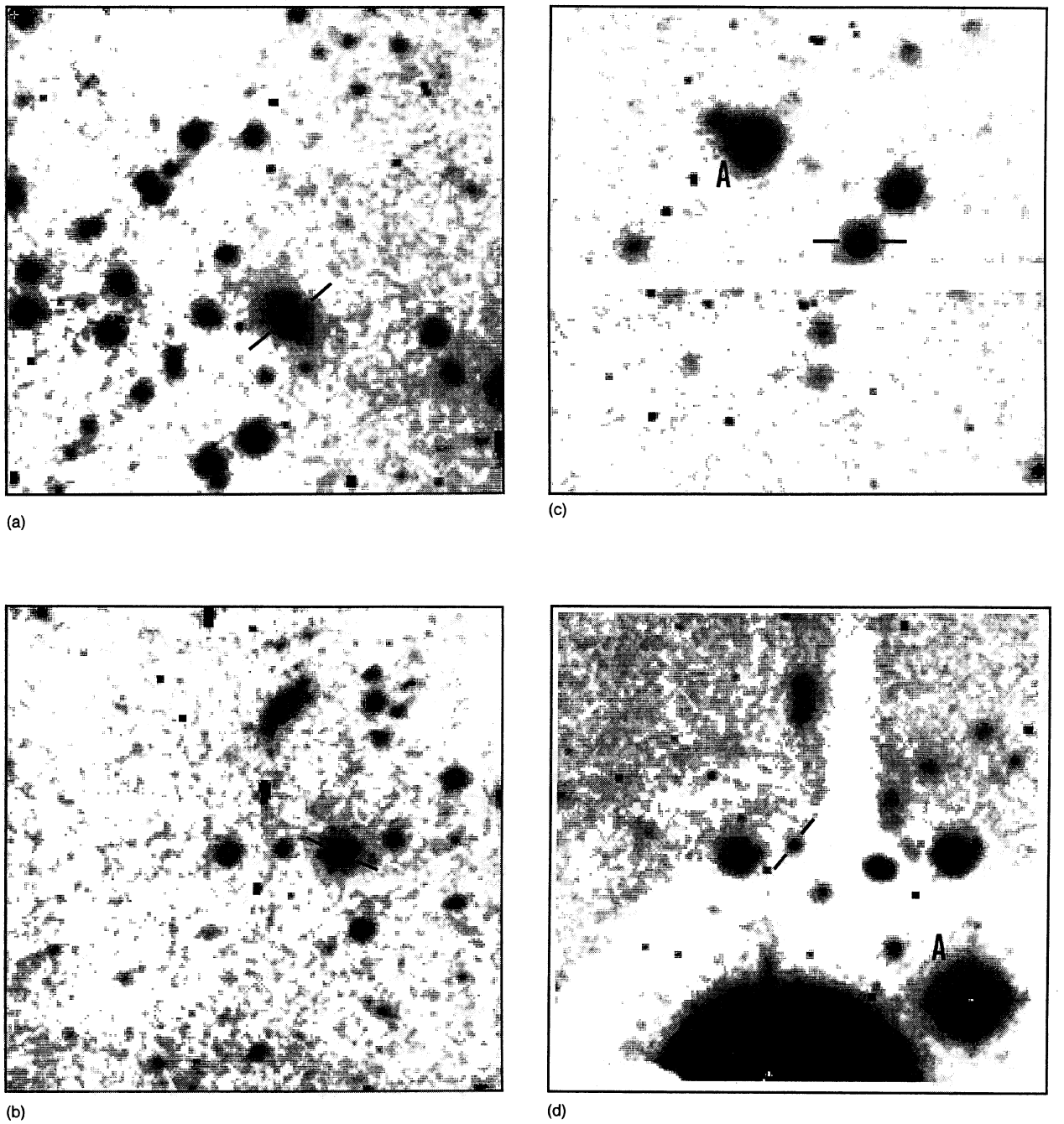

FIG. 2. (a)–(d) Optical *r* band images of 2038 – 280, 2039 – 232, 2116 – 250, and 2132 – 236. The size of each image is 65″ × 65″ and the identification is marked with two ticks whose orientation reflects that of the extended radio source. A secondary reference star is marked with an "A" in each field except for those in which the offset star lies outside the area shown. (e)–(h) *r* images of 2224 – 273, 2227 – 214, 2247 – 232, and 2318 – 244. (i)–(l) 0140 – 257, 0152 – 209, 0254 – 274, and 0324 – 228, the field size for 0254 – 274 is 125″ × 125″. (m)–(p) 0325 – 260, 0349 – 211, 0406 – 244, and 0407 – 226.

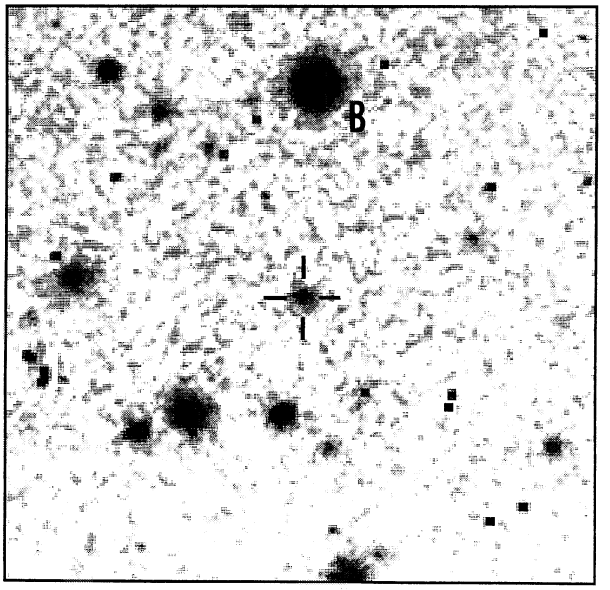

(e)

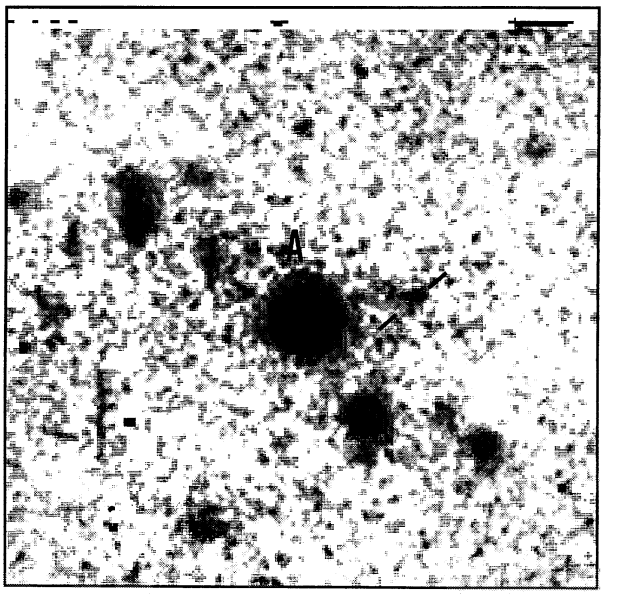

(g)

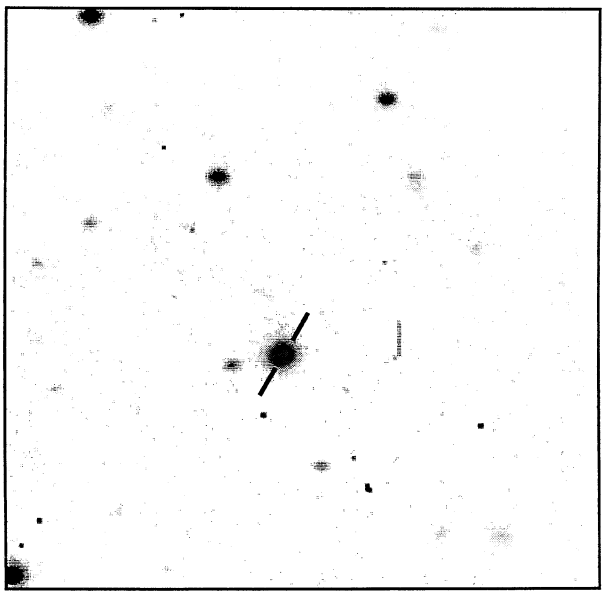

(f)

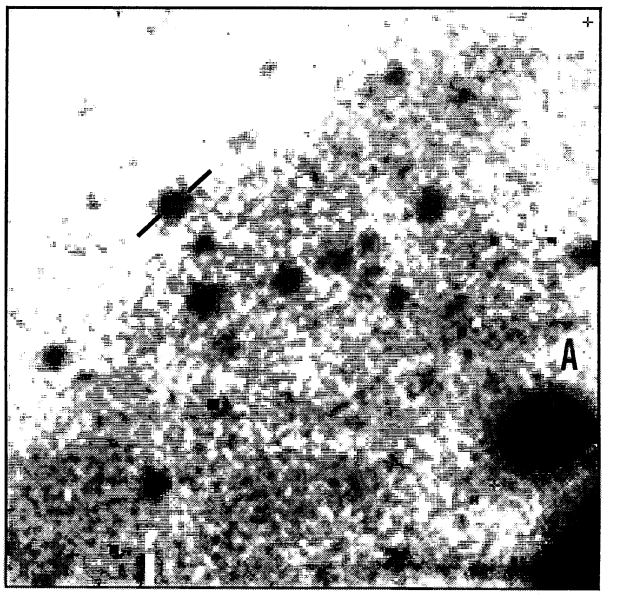

(h)

FIG. 2. (continued)

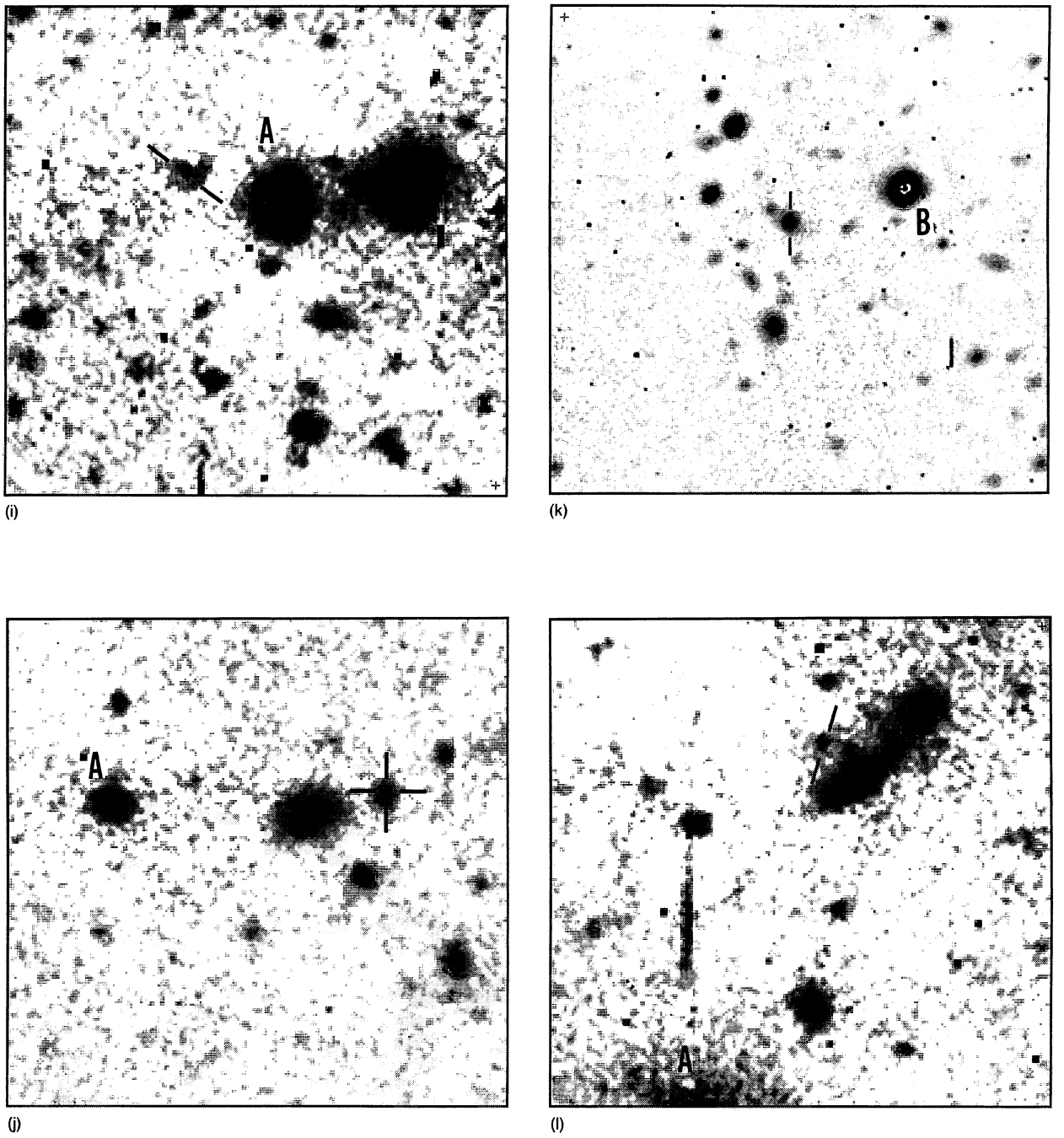

FIG. 2. (continued)

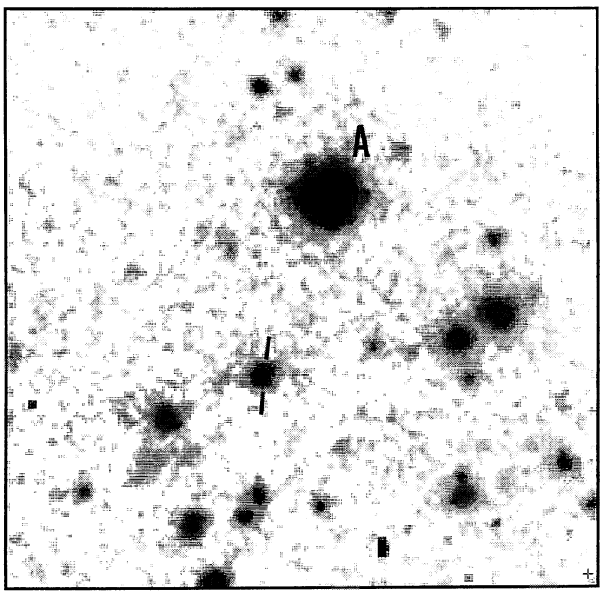

(m)

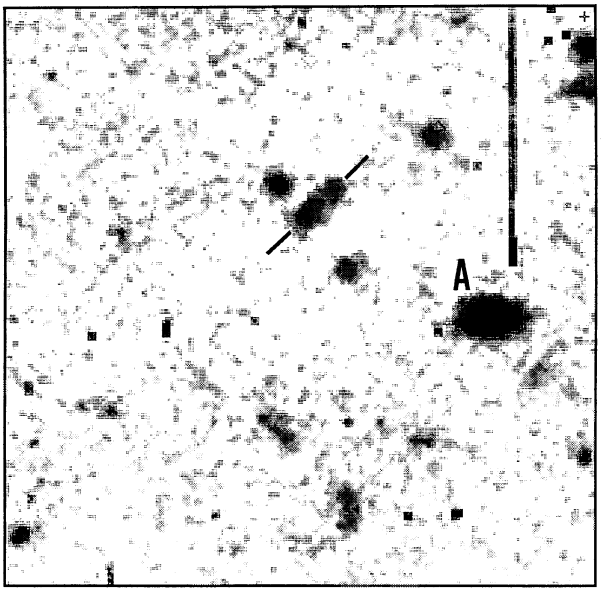

(o)

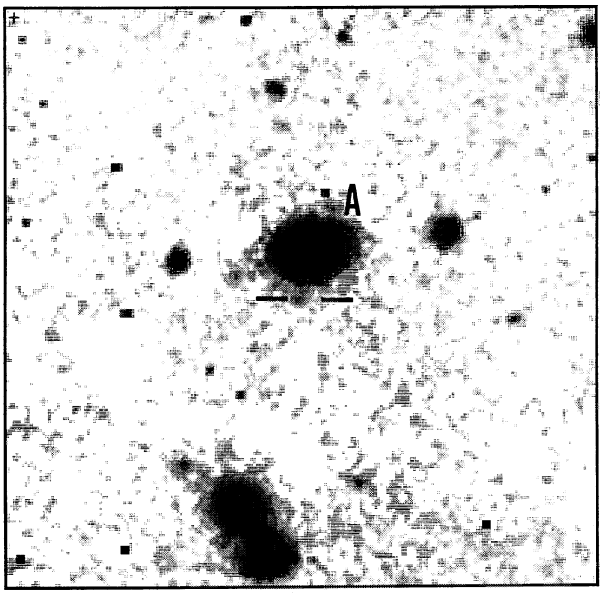

(n)

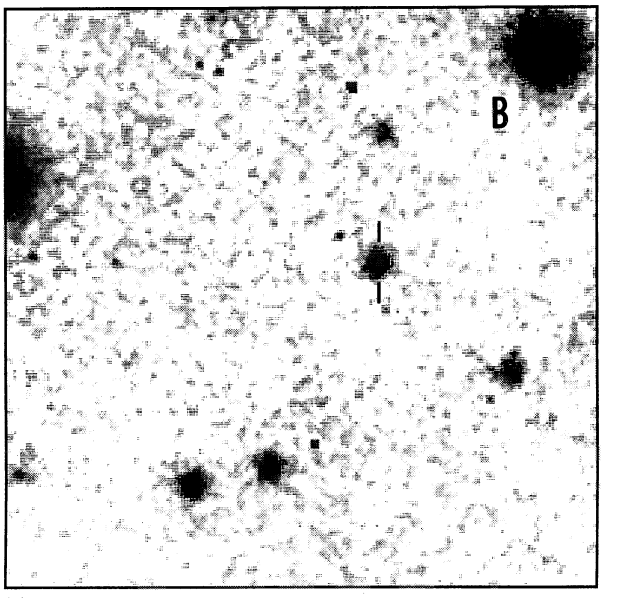

(p)

FIG. 2. (continued)

Spectrograph. We used a 150 ℓmm^{-1} grating blazed at 5000 Å with a Texas Instruments 800×800 CCD. The wavelength range covered went from 5400 to 9200 Å with an average pixel size of 4.7 Å×0.8″ and 15 Å resolution. Integration times were typically 3000 s.

The data were processed and calibrated using standard techniques and 2 d sky subtracted spectra were produced for each observation. One-dimensional spectra were extracted with a typical aperture size of 3″.5. After flux calibration the centroids, equivalent widths, and (when possible) fluxes of each of the emission lines were determined. The emission lines detected in each object are detailed below and in Table 3.

3. RESULTS

Notes on individual objects:

2038—280. This is the largest radio source in our sample (150″; 1.05 Mpc). Most of the radio structure is resolved out in our 6 cm A/B array observations. The source is identified with a moderately faint galaxy with weak [O II] 3727, [O III] 5007, 4959, and Hβ at a redshift of 0.39. The galaxy seems to lie in a fairly rich cluster.

2039—232. This galaxy is the brightest member of a loose cluster. The radio source is a fairly large (45″; 400 kpc) asymmetric double with a weak core and a possible jet extending to the northeast. A long slit spectrum in the red revealed strong [O III] 5007, 4959, and Hβ at a redshift of 0.621.

2116—250. The galaxy is quite compact. Our deep r image, taken in 1.4″ seeing shows it to be marginally resolved. The radio source is a highly asymmetric triple with the south eastern lobe lying three times further from the core than the north western lobe and having a very compact hot spot. Spectra taken with both the Du Pont telescope (red) and the CTIO 4 m (blue) showed strong [O III] 5007, 4959, Hβ, [O II] 3727, [Ne III] 3869, 3963, and [Ne V] 3426, 3323 at a redshift of 0.467. No broad Hβ was detected in our red spectra, but the signal-to-noise ratio was not very high.

2118—266. This bright cluster galaxy is identified with a moderately large (33″; 215 kpc), very asymmetric radio source with a very strong core. Any radio emission opposite of the eastern lobe is fainter than $\lesssim$0.5 mJy. Our red spectra revealed moderately strong emission from Hα and [N II] 6843, 6483 at a redshift of 0.343.

2132—236. This faint galaxy lies near the center of a large (55″; 550 kpc) simple double. The galaxy is not particularly extended but has strong emission from [O II] 3727 and [O III] 5007, 4959 at a redshift of 0.81. We also detected weaker lines that we identify as [Ne III] 3869 and [Ne V] 3426.

2224—273. This faint galaxy is identified with a very small (0.4″; 5.0 kpc) steep spectrum radio source. A long slit spectrum taken in the blue with the CTIO 4 m telescope revealed strong emission from Ly α, C IV 1549, C III] 1909, and weak He II 1640 at a redshift of 1.679. The equivalent width of Ly α (350 Å) is rather large for the 1 Jy sources.

2227—214. This is the only bona fide quasar in this current sample of sources.

2247—232. This $r = 24.5$ galaxy is one of the faintest in our sample. The image is extended and is aligned with the radio source, which is a 9.3″ (111 kpc) double. Two 4000 s spectroscopic observations with the CTIO 4 m revealed weak emission lines that we identified as C III] 1909 and C II] 2326 at a redshift of 1.33. This is one of the weakest lined objects in our sample.

2318—244. This galaxy is not particularly extended in our deep r band image. A single 3000 s spectroscopic observation with the CTIO 4 m revealed a rich emission line spectrum as is shown in Fig. 3(a). We detected six emission lines that we identify as C IV 1549, He II 1640, C III] 1909, C II] 2326, [Ne III] 2424, and Mg II 2800 at a redshift of 1.113. There appears to be a weak broad component to the Mg II emission line, but high quality spectra are needed to confirm this.

2321—228. This galaxy is the central member of a group of three bright galaxies easily visible on the sky survey. For this reason we did not image it with the 2.5 m. A red spectrum taken with the 2.5 m revealed weak Hα and [N II] 6584, 6548 emission at a redshift of 0.114. The radio source is asymmetric, with low surface brightness lobes. Much of the source structure is resolved out with our resolution.

0140—257. This faint galaxy is spatially extended and is aligned with the axis of its small (3.4″; 46 kpc) double radio source. One 3000 s spectrum with the 4 m revealed a single line that we identify as Ly α at a redshift of 2.63. The only other plausible identifications for this line are [O II] 3727 at $z = 0.18$ and C III] 1909 at $z = 1.31$, the first being highly unlikely given the faintness of the object and the small scatter in absolute magnitudes of radio galaxies at intermediate redshifts (e.g., Hill & Lilly 1991). If the line at 4414 Å were C III] 1909, then we should easily have detected C IV 1549 at 3580 and C II] 2326 at 5378. The significant drop in the continuum to the blue of the 4414 Å emission line and its large equivalent width reinforce our identification with Ly α.

0152—209. This galaxy is not particularly extended and is also identified with a small (0.6″; 7.7 kpc) steep spectrum source. Two 3000 s observations with the CTIO 4 m revealed four emission lines that we identify as Ly α, C IV 1549, He II 1640, and C III] 1909 at a redshift of 1.920.

0254—274. This intermediate redshift galaxy lies at the center of a rich cluster. Our red spectra with the 2.5 m reveal a strong 4000 Å break and weak ($W_\lambda = 45$ Å) [O II] 3727 emission at a redshift of 0.49. At radio wavelengths we detect only a faint, slightly resolved central radio component. All the extended radio structure is resolved, there is some evidence for twin jets north and south of the galaxy.

0324—228. This faint galaxy appears rather small in our r image, but is contaminated by a foreground spiral a few arcseconds away. The radio source is a 9.5″ (122 kpc) double without a core. Our blue spectrum obtained with the 4 m reveals four emission lines that we identify as Ly α, C IV 1549, He II 1640, and C III] 1909 at a redshift of 1.894. The equivalent width of Ly α is quite large ($>$900 Å).

0325—260. This intermediate brightness galaxy is only moderately extended in our deep r image. A red spectrum obtained with the 2.5 m revealed four emission lines that we identify as [O II] 3727, Hβ, [O III] 5007, 4959 at a redshift of 0.638. The radio source is rather large (59″; 537 kpc), with no evidence for a radio core. Most of the source structure is resolved out.

0349—211. This faint galaxy is quite compact in our deep r image and is coincident with the core of a small (7.1″; 94 kpc) triple source. Our blue spectrum [Fig. 3(b)] taken with the 4 m shows strong narrow Ly α emission and weaker emission from C IV 1549, and possibly S IV/O IV 1400. These weaker lines are broader than in typical high redshift radio galaxies and Ly α appears to have a broad base. This is

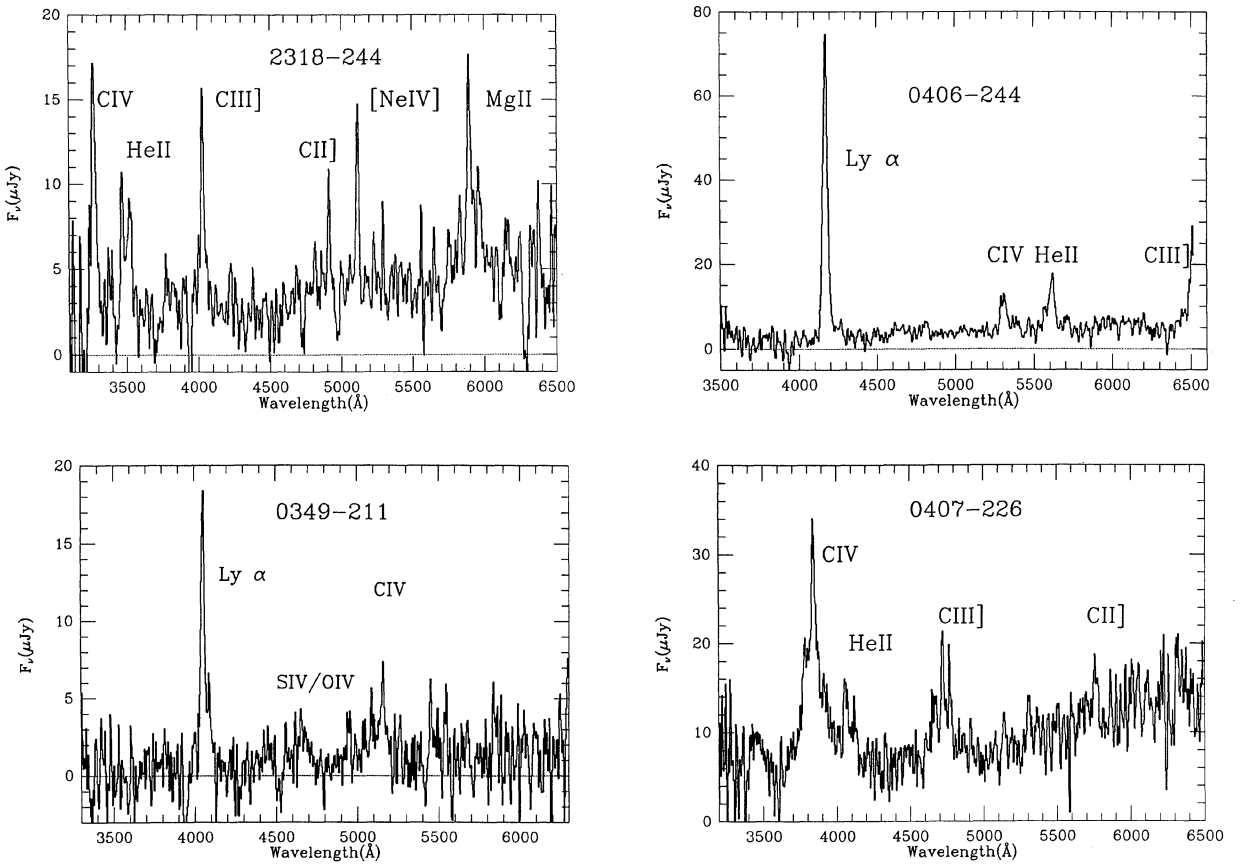

FIG. 3. Spectra of 2318 − 244, 0349 − 211, 0406 − 244, and 0407 − 226. All of these spectra were taken with the CTIO 4 m and its folded-Schmidt spectrograph. The strongest emission lines are marked.

one of a few galaxies that we tentatively label as high redshift broad line radio galaxies, but high quality spectra are needed to confirm the line profiles.

0406−244. This is the most spectacular object in the current subsample. The galaxy has two distinct components that are separated by 4″ and are coincident with the core and northwest lobe of the radio source. The source has a weak but well detected core that is fairly far from the center of the two lobes. Long slit spectra taken with the slit aligned along the two components of the galaxy (or two galaxies) with the 4 m revealed very strong and spatially extended emission lines that we identify as Ly α, C IV 1549, He II 1640, and C III] 1909 at a redshift of 2.427. The spectrum is shown in Fig. 3(c). All of the emission lines extend along the slit in the direction of the southern radio lobe. The northern galaxy shows no strong emission lines in our spectra. The southern radio lobe is the closer of the two lobes and is also the side of the brightest emission lines. McCarthy *et al.* (1991) show that in the 3CR there is a nearly universal correlation between the side of the closer radio lobe and the side of the brightest emission lines.

0407−226. This object is extremely compact in our *r* image and is coincident with the core of a 23″ (281 kpc) double source. A single spectrum [Fig. 3(d)] with the 4 m revealed strong emission lines from C IV 1549 and C III] 1909 as well as weaker He II 1640 and S IV/O IV 1400 at a redshift of 1.49. The C IV and C III] emission lines clearly have multiple component profiles with narrow cores superposed on broad bases. He II shows only a narrow profile, while S IV/O IV 1400 shows only a broad component. The relative line strengths of the broad components of C IV and C III] (2:1) are typical of quasars while the narrow line spectrum looks quite typical of high redshift radio galaxies. This object appears to be a high redshift example of a broad line radio galaxy. The continuum is also unusually bright for this redshift suggesting a substantial non-stellar contribution.

4. DISCUSSION

4.1 The Identification Content of the Survey

The imaging observations of our original sample of 120 sources are now more than 90% complete. Thus we can make a fairly accurate determination of the identification content of the survey. Our VLA A/B array maps are inadequate for six of the sources due either to confusion or, in most

cases, because of missing large scale structure. We have deep optical images for 105 of the 114 remaining sources. Of these 86% (91/105) are identified with galaxies, 8% (8/105) are quasars and the remaining 6% (6/105) are unidentified ($m_r \gtrsim 25$) after 2700 s or more of imaging with the Du Pont 2.5 m telescope at Las Campanas Observatory. Of the galaxies, 11% (12/105) are in rich cluster at modest redshifts (0.1–0.6). Most of these are visible on the sky survey but had not been identified because the MRC positions are inaccurate for these large diffuse sources. The remaining 68 galaxies are quite faint and are likely to lie at moderately large redshifts. The small fractional quasar content of our sample results both from the steep spectrum selection and the exclusion of sources identified on the sky survey films. The quasars identified on the sky survey from the parent sample of 700 sources are being observed in a separate program by Kapahi, Hunstead, and Subrahmanya.

The median redshift of the 31 objects for which we currently have spectroscopy is 1.2. This is likely to increase since nearly all of the bright identifications have now been observed spectroscopically. Excluding the sources that should have been identified on the sky survey, our median redshift is ~ 1.5. The range of redshifts spanned by our sample makes it well suited for comparison to earlier samples (e.g., 3CR and B2/1Jy) as well as to examine the redshift dependencies of the alignment effect and the spectral energy distributions of the galaxies, both of which undergo strong changes near $z \sim 1$.

4.1.1 The emission line luminosity versus radio power correlation

One of the motivations for this survey of intermediate flux density sources was to examine the relations between the emission line and radio luminosities in sources less luminous than the 3CR sources in the same redshift range. A number of investigations have revealed correlations between emission line luminosity and radio luminosity in low redshift samples (Baum & Heckman 1989b; Saunders *et al.* 1990). Using the complete 3CR McCarthy & van Breugel (1989) found a strong correlation between the [O II] 3727 emission line luminosity and the radio luminosity over the entire range of luminosities in the 3CR sample. The strong but artificial correlation between radio power and redshift in the 3CR, however, makes it impossible to distinguish between a

TABLE 3. Photometric data.

IAU Name	z	r	f(Line)	W_λ(rest)	L(Line)	Line
2038-280	0.390	20.51	-	69 ± 30	-	[OIII]3727
			-	5 ± 1	-	[OIII]5007
2039-232	0.621	20.4	11	74 ± 11	42.41	[OII]3727
			66	187 ± 13	42.78	[OIII]5007
2116-250	0.458	19.17	23	78 ± 7	42.41	[OII]3727
			187	285 ± 8	43.32	[OIII]5007
2118-266	0.343	-	-	29 ± 13	-	[OII]3727
			-	35 ± 5	-	[OIII]5007
2132-236	0.81	22.31	9	90 ± 80	42.61	[OII]3727
2224-273	1.679	22.51	47	347	44.20	Ly α
2227-214	1.391	18.71	89	39	44.25	CIV 1549
2247-232	1.326	24.2	1.5	25 ± 15	42.39	CIII]1909
2318-244	1.113	23.0	7	68 ± 28	42.85	CIII]1909
2321-228	0.114	-	-	38 ± 2	-	Hα
0140-257	2.616	23.5	3	85 ± 49	43.65	Ly α
0152-209	1.920	23.17	18	190 ± 63	43.95	Ly α
0254-274	0.48	19.70	10	30 ± 11	42.11	[OII]3727
0324-228	1.894	23.9	20	> 300	43.98	Ly α
0325-260	0.638	22.2	-	119 ± 56	-	[OII]3727
			-	183 ± 54	-	[OIII]5007
0349-211	2.329	24.7	9	187 ± 67	43.92	Ly α
0406-244	2.427	22.4	47	418 ± 80	44.69	Ly α
0407-226	1.474	21.8	67	295	44.19	CIV 1549

primary correlation between $L([\mathrm{O\ II}])$ and redshift and a correlation between $L([\mathrm{O\ II}])$ and $L(\mathrm{radio})$. Our sample of 1 Jy Molonglo sources, with a wide range of redshift overlap with the 3CR allows a better determination of the reality of the $L([\mathrm{O\ II}])$ vs $L(\mathrm{radio})$ correlation. We have used the line strengths and radio flux densities and spectral indices given here, in Paper I, and for a similar sample of 1 Jy sources drawn from the B3 catalog given by McCarthy (1991) to compute emission line luminosities and radio powers and luminosities. We have also included a few objects from the B2/1 Jy sample of Allington-Smith *et al.* (1988). For this particular comparison we have used the following cosmological parameters, $H_0 = 50$, $q_0 = 0$, and $\Lambda = 0$. The choice of cosmology, however, is inconsequential to the test for a primary $L([\mathrm{O\ II}])$ vs $L(\mathrm{radio})$ correlation. In computing the equivalent [O II] 3727 line luminosities we have scaled the observed line strengths (Ly α, C III] 1909, [O III] 5007) using the same line ratios that were derived from the 3CR sample as given in McCarthy, Spinrad and van Breugel (1991) and McCarthy (1988).

In Fig. 4(a) we plot the emission line luminosity against the radio power for the 3CR and 1 Jy samples. The open symbols refer to the 3CR sample of McCarthy *et al.* (1991) while the filled symbols are for the 1 Jy sources. For the $\log L([\mathrm{O\ II}]) - \log P(1400)$ correlation we find a regression coefficient for the combined sample of 0.88 and a least-squares best-fitting slope of 0.92 ± 0.04. Using the 1 Jy samples alone we find a regression coefficient of 0.84 and a slope of 0.88 ± 0.12. In Fig. 4(b) we plot $\log L([\mathrm{O\ II}])$ against $\log(1+z)$. Comparison between Figs. 4(a) and 4(b) shows clearly that the primary correlation is between emission line luminosity and radio power (and hence luminosity) rather than redshift. We have used the radio powers in our test rather than the luminosities because these are better defined with our limited spectral coverage in the radio. An analysis using the radio luminosities derived from the spectral indices at 1400 MHz gives similar results but with slightly more scatter. This result bears strongly on our understanding of the origin and ionization of the extended emission line regions. The correlation between $L([\mathrm{O\ III}]\ 5007)$ and $L(\mathrm{radio})$ at low redshifts has been used to argue in favor of models in which the extended emission line regions are photoionized by the active nucleus (e.g., Baum & Heckman 1989b; van Breugel & McCarthy 1989) and have been taken as evidence in support of the unifying models of AGNs as discussed by Barthel (1988).

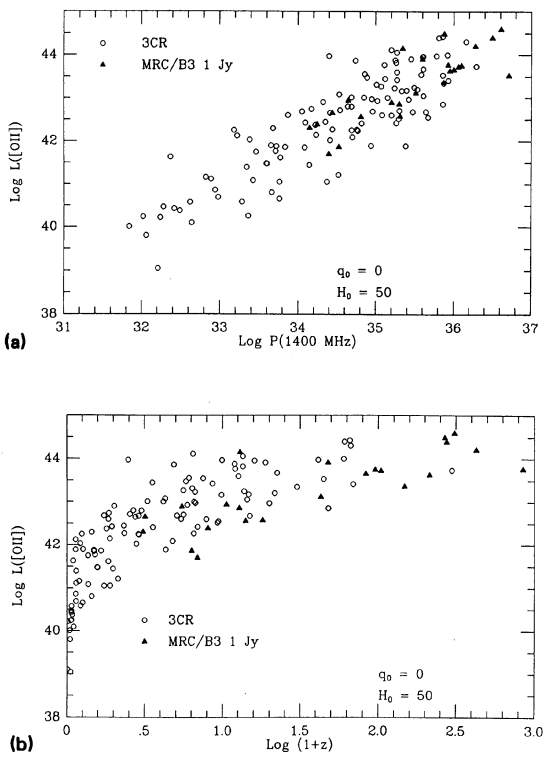

FIG. 4. (a) The log of the equivalent [O II] 3727 emission line luminosity plotted against the log of the radio source power at 1400 MHz for the 3CR sample (open symbols) and the 1 Jy samples (filled symbols). (b) The equivalent [O II] 3727 emission line luminosity plotted against $\log(1+z)$.

4.1.2 The structure of the sources

The structure of the sources mapped in this investigation appear to differ in some respects from those found in the 3CR sample at high redshift and run counter to expectations based on the source selection criteria. The 3CR galaxies at large z are nearly all simple double sources. Most have weak cores, and a large fraction ($\sim 25\%$) do not have detected cores at the 0.5 mJy level (Laing *et al.* unpublished). Few, if any, of the high redshift 3CR galaxies have jetlike radio structures. The MRC sources presented here and in Paper I, however, differ in that a large fraction of them have moderately strong cores and structures that are not simple doubles.

A surprisingly large number of sources are very large. There are four sources at moderately large redshifts ($0.3 \lesssim z < 0.8$) with linear sizes $\gtrsim 0.5$ Mpc. Wiita & Gopal-Krishna (1987) have suggested that giant radio galaxies (GRGs; $D_{\max} > 1.5$ Mpc for $H_0 = 50$), may be caused either by moderately powerful long-lived AGN or by very powerful but relatively short lived nuclei. They prefer the latter explanation because of the moderately high radio powers (just above the break in the radio luminosity function), rarity, and relatively large core/lobe ratios in the giant sources. On the basis of their models Wiita & Gopal-Krishna predict a significant number of GRGs in the redshift range $0.2 \lesssim z \lesssim 0.6$. The four largest sources in our sample are not quite of the 1.5 Mpc class but since we found several of them in the current subsample it is of interest to see how their radio properties compare with genuine GRGs. All of the sources in our sample, which was selected to include a large fraction of distant radio galaxies, have radio powers well above the break in the luminosity function at $P_{1.4,\mathrm{rest}} \gtrsim 10^{33}$ ergs s^{-1} cm^{-2} Hz^{-1}. We do not, however, find strong radio cores in the largest sources, although their redshifts are relatively large, in agreement with the Wiita/Gopal-Krishna prediction. The core/total flux density ratios in the largest sources are small, typically $\lesssim 1.5\%$.

Of the 17 sources in our sample currently known to have redshifts greater than one, five are simple doubles, three are compact doubles, and the remaining nine all have moderately strong cores, two of these being unresolved at the 1″ level. The objects with strong cores still have steep radio spectra. The strong cores are of interest in light of the unifying mod-

els of radio galaxies and quasars (Orr & Browne 1982; Barthel 1988; Kapahi 1989). In these models the cores of powerful radio sources are strongly beamed and hence their visibility is strongly dependent on the angle to the line of sight. The Doppler factors derived for QSRs from superluminal motion studies (e.g., Cohen *et al.* 1989) imply $\gamma \sim 10$–20, while the less luminous sources require $\gamma > 2$. The relative angular sizes and redshift distributions of radio galaxies and QSRs in the 3CR catalog led Barthel to conclude that an angle to the line of sight of $\sim 45°$ defined the division between the optical signatures of quasars and radio galaxies. The range of angles over which these sources show the *radio* signatures of a quasar (bright jets, strong cores, superluminal motion) are somewhat smaller as they are related to Doppler boosting rather than obscuration. Thus in the Barthel version of the unified scheme it is possible to see an object with the optical signature of quasar, but without the strong radio signature of a beamed object. These objects are identified with the "Broad Line Radio Galaxies" (Osterbrock *et al.* 1975). It is interesting to note in this respect that at one of our strong core sources, 0407 − 226, indeed appears to be a BLRG. The other objects (except possibly 0349 − 211), including the two unresolved objects have no evidence for broad lines and are quite faint in the continuum. High resolution maps of the radio galaxy 0902 + 34 at $z = 3.4$ (Lilly 1988) show a strong core and a bright one-sided jet (van Breugel & McCarthy 1989). From a purely radio perspective, 0902 + 34 and a number of the objects presented here and in Paper I (e.g., 2247 − 248, 2224 − 273, 2318 − 244, 0349 − 211, and 0152 − 209) could be classified as quasars, yet none of them show the compact optical structure and broad emission lines characteristic of such objects. Explaining the radio and optical properties of these objects may pose a problem for the simplest versions of the unifying scheme.

We would like to thank the staffs of the Las Campanas, National Optical, and National Radio Astronomy Observatories for their expert assistance with the observations. V. K. K. acknowledges the support of a National Research Council–JPL Senior Research Associateship under which part of this research was carried out. The National Radio Astronomy Observatory and the VLA are operated by Associated Universities, Inc., under a contract with the National Science Foundation. The National Optical Astronomy Observatory and the Cerro Tololo Inter-American Observatory are operated by AURA, Inc., under a contract with the National Science Foundation. The Las Campanas Observatory is owned and operated by the Carnegie Institution of Washington.

REFERENCES

Allington-Smith, J. R. 1982, MNRAS, 199, 611
Allington-Smith, J. R., Spinrad, H., Djorgovski, S., and Liebert, J. F. 1988, MNRAS, 234, 1091
Barthel, P. D. 1989, ApJ, 336, 606
Baum, S. A., and Heckman, T. M. 1989, ApJ, 336, 681
Chambers, K. C., Miley, G. K., and van Breugel, W. J. M. 1987, Nat, 329, 604
Chambers, K. C., and Miley, G. K. 1990, in The Hubble Centennial Symposium: The Evolution of the Universe of Galaxies, edited by R. G. Kron, (PASP Conference Series No. 10), p. 373
Chambers, K. C., Miley, G. K., and van Breugel, W. J. M. 1990, ApJ, 363, 21
Dunlop, J. S., Peacock, J. A., Savage, A., Lilly, S. J., Heasley, J. N., and Simon, A. J. B. 1989, MNRAS, 238, 1171
Eisenhardt, P., and Chokshi, A. 1990, ApJL, 351, L9
Hill, G., and Lilly, S. J. 1991, ApJ, 367, 1
Kaphi, V. K. 1990, in Parsec Scale Radio Jets, edited by J. A. Zensus and T. J. Pearson (Cambridge University Press, Cambridge), p. 304
Laing, R., Owen, F., and Puschell, J. (unpublished)
Large, M. I., Mills, B. Y., Little, A. G., Crawford, D. E., and Sutton, J. M. 1981, MNRAS, 194, 693
Lawrence, C. R., Bennett, C. L., Hewitt, J. N., Langston, G. I., Klotz, S. E., and Burke, B. F. 1986, ApJS, 61, 105
Lilly, S. J. 1988, ApJ, 333, 161
Lilly, S. J. 1989, ApJ, 340, 77
McCarthy, P. J., Kapahi, V. K., van Breugel, and Subrahmanya, C. R. 1990, AJ, 100, L29
McCarthy, P. J., Spinrad, H., and van Breugel 1989, in The Structure and Evolution of Active Galactic Nuclei, edited by D. E. Osterbrock and J. Miller (PASP, Conference Series), p. 543
McCarthy, P. J., van Breugel, W. J. M., and Kapahi, V. K. 1990, ApJ, 100, 1014 (Paper I)
Orr, M. J. L., and Browne, I. W. A. 1982, MNRAS, 200, 1067
Osterbrock, D. E., Koski, A. T., and Phillips, M. M. 1975, ApJ, 197, L41
Saunders, R., Baldwin, J. E., Rawlings, S., Warner, B., and Miller, L. 1989, MNRAS, 238, 777
Strom, R. G., Riley, J. M., Spinrad, H., van Breugel, W. J. M., Djorgovski, S., Liebert, J. F., and McCarthy, P. J. 1990, A&A, 227, 19
van Breugel, W. J. M., and McCarthy, P. J. 1990, in The Hubble Centennial Symposium: The Evolution of Galaxies, edited by R. G. Kron (PASP, Conference Series) (in press)
Wiita, P. J., and Gopal-Krishna 1987, in Active Galactic Nuclei, edited by H. R. Miller and P. J. Wiita, Lecture Notes in Physics (Springer, Berlin)